Meas. Sci. Technol. **18** (2007) 2320–2327 doi:10.1088/0957-0233/18/8/005

Measurements for low level RF control systems

S N Simrock

DESY, Notkstr. 85, 22607 Hamburg, Germany

E-mail: stefan.simrock@desy.de

Received 6 December 2006, in final form 13 March 2007
Published 6 July 2007
Online at stacks.iop.org/MST/18/2320

Abstract
The low level RF control system for the European x-ray free electron laser, which is based on TESLA technology, requires information on a large number of signals and parameters which are either directly measurable as physical signals or must be derived from the physical signals. In most cases, calibrations are required to obtain the desired quantities. The measured signals are used in the real time feedback loops for field and resonance control, and for diagnostic purposes to support automation and exception handling. Good system models and powerful signal processors (including field programmable gate arrays and digital signal processors) combined with fast communication links allow for processing a large number of complex algorithms in real time. Several of these algorithms have been implemented at the free electron laser at Hamburg (FLASH) for evaluation and have increased the availability of the facility for user operation.

Keywords: rf control, rf system, superconducting accelerator, feedback, measurement

1. Introduction

The European x-ray free electron laser (XFEL) is a fourth-generation synchrotron radiation facility based on the SASE FEL concept and the superconducting TESLA technology for the linear accelerator. This multi-user facility will provide photon beams in a wavelength regime from 0.1 nm to 5 nm in three FEL beam lines and hard x-rays in two spontaneous radiation beam lines, serving in total ten experimental stations in the first stage. The project is in an advanced planning and technical preparation stage, and its construction as a European/International facility near DESY in Hamburg will start in 2007. The main parameters of the RF system of the linac are listed in table 1.

2. RF system

The RF control system for one RF station consisting of a 10 MW klystron driving 32 cavities in four cryomodules must provide control of the vector sum of all cavities with a stability of the order of 2×10^{-4} for amplitude and up to 0.01° in phase at 1.3 GHz. The feedback system requires individual field measurements from which the vector sum is calculated as well as forward and reflected power measurements from which cavity detuning and beam phase are derived and which are used for system diagnostics. To support a low latency in the feedback loop of less than 1 μs, 100 MHz ADCs with 14 bit resolution and DACs, both with few cycle conversion times and with a low latency processing unit based on large field programmable gate arrays (FPGAs), are required. The field detection is accomplished by downconversion of the cavity probe signal at 1.3 GHz to an IF frequency of about 50 MHz which is sampled by the ADC from which the field vector is calculated. A vector modulator driven by a DAC allows fast control of the incident power in amplitude and phase. Piezotuners support fast cavity tuning to compensate Lorentz force detuning. Beam-based feedback will be used to correct long-term drifts. The beam diagnostics include measurements of the energy using spectrometers, bunch compression and measurement of the arrival time of the beam at various locations.

3. Measurement and control signals

The LLRF control system [1, 7, 8] requires information on a large number of signals and parameters which are either

 © 2007 IOP Publishing Ltd Printed in the UK

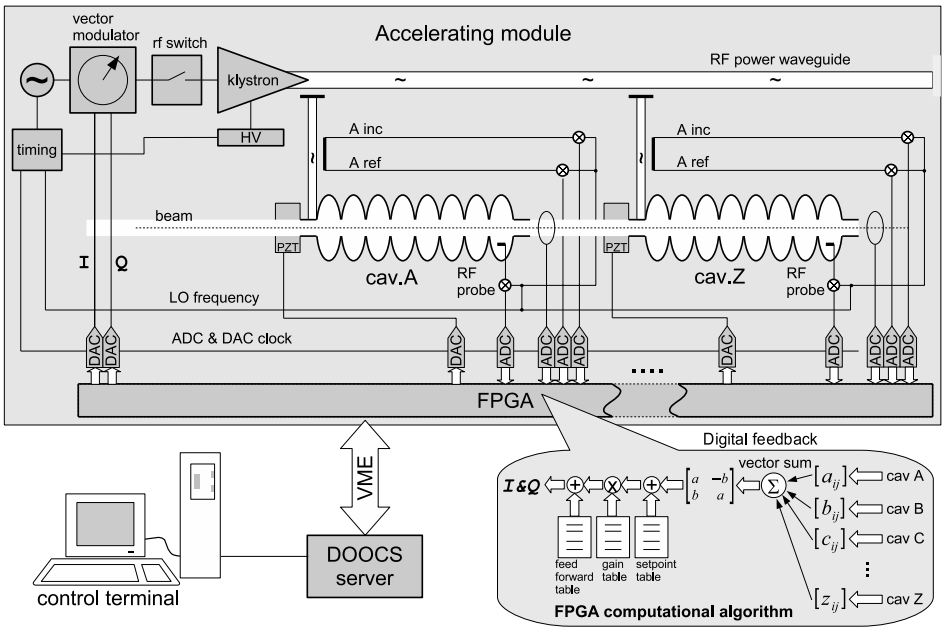

Figure 1. Architecture of a typical RF system.

Table 1. Parameters of the main linac of the European XFEL.

Parameter	Value
Energy for 0.1 nm wavelength (maximum design energy)	17.5 GeV (20 GeV)
Number of installed accelerator modules	116
Number of cavities	928
Acc. gradient (104 active modules) at 20 GeV	23.6 MV m^{-1}
Number of installed RF stations 29 Klystron peak power (26 active stations)	5.2 MW
Loaded quality factor Q_{ext}	4.6×10^6
RF pulse length	1.4 ms
Beam pulse length	0.65 ms
Repetition rate	10 Hz
Maximum number of bunches per pulse (at 20 GeV)	3250
Minimum bunch spacing	200 ns
Bunch charge	1 nC
Bunch peak current	5 kA
Emittance (slice) at undulator	1.4 mm mrad
Energy spread (slice) at undulator	1 MeV

directly measurable as physical signals or are not directly measurable but must be derived from the direct measurements. In most cases, calibrations are required. The architecture of the RF system planned for the European XFEL [2, 3] is shown in figure 1.

The physical signals available at the European XFEL are as follows.

- *Cavity probe signal at 1300 MHz.* The cavity probe signal represents a sample of the cavity field measured with an antenna which is loosely coupled to the end cell opposite the input coupler. Due to the strong cell-to-cell coupling of the order of several per cent, the signal is proportional to the voltage $V_0 \cdot \cos\phi$ experienced by the beam when traversing the cavity.
- *Cavity probe signal at the IF frequency after downconversion.*
- *Forward and reflected power of individual cavities, at the output of the klystron, and at the output of the vector modulator and the RF preamplifiers.* Samples of the forward and reflected power signals are available at the ports of a directional coupler inserted in the waveguide close to the cavity input power coupler. The signal must be corrected for the complex directivity which describes the crosstalk from the reflected power into the forward power port and the forward power into the reflected power port.
- *Forward and reflected power signals at the IF frequency after downconversion.*
- *Single bunch transient output of the transient detector.* The single bunch transient detector measures the amplitude and phase of the beam-induced transient of a single bunch. Since the transients are very small compared to the RF field (of the order of a few 1×10^{-4}) and must be measured with a resolution of a few per cent, the overall resolution must be of the order of 1×10^{-5}.
- *Fast tuner piezoactuator and sensor signal.* The fast tuner is based on a piezoelectric actuator which changes its length when a voltage is applied to the electrodes. This

length change is mechanically transferred to the cavity which in turn is deformed, thereby changing the resonance frequency. The actuator is integrated into the motor tuning system. The function of a second piezoelectric stack is to produce a voltage proportional to the deformation change of the cavity.

- *Motor tuner position for frequency tuners.* The frequency tuner is driven by a stepper motor. For the position measurement, only the total number of motor steps is recorded from which a frequency change from a reference position can be calculated.
- *Waveguide tuner stub positions.*
- *Vector-modulator drive signal.* The vector modulator has two inputs (I and Q) which allow us to control the in-phase (I) and quadrature (Q) components of the incident wave to the cavity. Since a sign change at the input changes the phase by 180°, one can achieve control in all four quadrants including zero.
- *HV pulse from the klystron modulator.* The measurement of the high voltage (HV) pulse shape of the klystron is important since klystron saturation power, klystron gain and klystron phase depend strongly on this parameter. For the 10 MW L-band multibeam klystron the phase sensitivity is 14° kV^{-1} and the saturation power changes by 2.5% kV^{-1}. This signal will be used to correct the feedforward table according to the measured high voltage.
- *Beam current from toroids.* The beam current measurement (amplitude and phase) will be used to compensate beam loading variations in real time with a delay of only a few μs. The information can be read by an ADC channel or sent to the controller board via optical link.
- *Beam diagnostic signals (bunch length, bunch energy, bunch arrival time from special diagnostics).* These signals are used to correct for slow drifts in amplitude and phase of various RF systems such as RF gun, pre-accelerator, injector linac, harmonic system or the booster section. The diagnostics must be implemented in such a way that it is possible to derive which of the amplitudes or phases has changed.
- *LO amplitude and phase.* The LO amplitude and phase are monitored to provide warnings or alarms in the case of deviations from the nominal value and to implement correction schemes where possible.
- *Calibration reference signal.* This signal is added to each probe and forward/reflected power signal. It will be a pulsed signal which is active a few ms before the actual RF pulse. The signal provides a phase and amplitude reference for each channel. The amplitude and phase of this signal must be highly stable.

From these signals—mainly from the probe, forward and reflected power—the following measurement signals can be derived.

- *Field vector from the sampled IF signal.* The field vector can be calculated from subsequent samples since the intermediate frequency and the sampling frequency are known and synchronized with the master oscillator. If more than two samples are used for the field calculation, it is possible to remove offsets or even correct for down-converter nonlinearities.
- *Cavity gradient and phase from forward and reflected power.* It is possible to calculate the cavity gradient from forward and reflected power and verify the consistency with the probe measurement.
- *Loop phase and loop gain (time varying).*
  - Loop phase and loop gain are essential parameters for the feedback stability and error suppression. They can be derived from the vector-modulator drive signal and the measured vector sum.
- *Loaded Q and cavity detuning (time varying).* The loaded Q and cavity detuning can be derived from the probe and forward/reflected power signals by solving the differential equation for the unknown parameters. The loaded Q must be set for efficient RF power transfer to the beam, and the detuning must be kept small to minimize the power needed for control.
- *Calibration parameters for cavity phase, and gradient and forward and reflected waves.* The measured field vectors are calibrated by scaling the amplitude and adding the correct phase offset. This is accomplished by multiplication with a rotation matrix. The calibration matrix is determined from the beam-induced voltage. This can be accomplished with single bunch transients or full beam loading.
- *Vector sum.* The vector sum is calculated as the sum of all calibrated cavity voltage vectors.
- *Beam current and beam phase.*
- *Exceptions such as cavity quench.*
- *RMS and peak error signals (gradient, phase).*
- *Average values, intra-pulse, pulse-to-pulse.*
- *Warnings and alarms.*

The following parameters can be extracted.

- Klystron saturation characteristics (amplitude and phase, calibrated gain).
- Down-converter characteristics (sensitivity, linearity, offset).

4. RF system hardware architecture

The main components of the RF system are shown in figures 1 and 2.

- Klystron with a preamplifier and HV modulator.
- Power transmission and distribution system with circulator, directional couplers and waveguide tuners.
- Cavity with couplers (in/out) and frequency tuners (slow/fast).
- LLRF system consisting of
  - downconverters to convert the 1300 MHz signals from probe/forward/reflected power to an IF in the 10–100 MHz range,
  - ADCs for digitization of the IF signals,
  - digital processing unit (FPGA, DSP, CPU),
  - DACs to drive the vector modulator and piezotuners,
  - vector modulator.

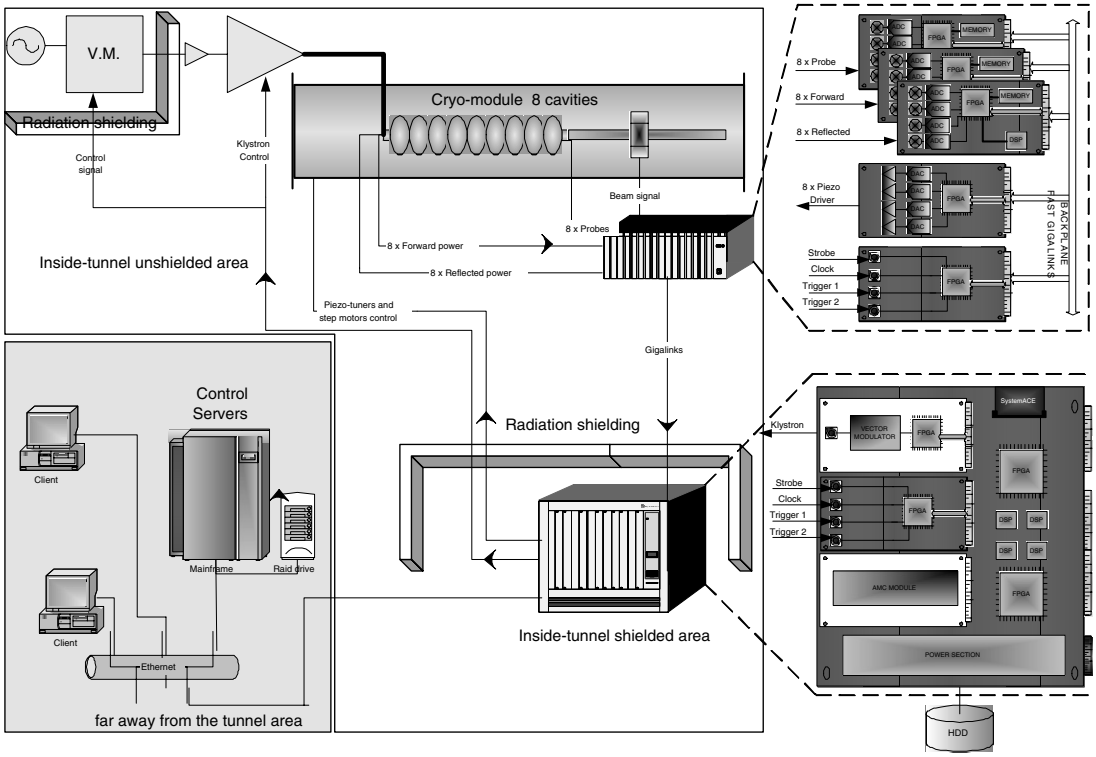

Figure 2. Hardware architecture of the RF system.

- RF reference signal for the vector modulator and LO signals. In addition, RF reference signals for calibration are needed.
- Timing signals (clocks and triggers).
- Control system interface.
- Interlock interface.
- Input from beam diagnostics (current, energy, etc).

The hardware configuration of the RF control loop is shown in figure 2.

The RF system signal flow is shown in figure 3. The cavity probe signal is converted from the cavity frequency of 1300 MHz to an IF frequency in the range of 10–100 MHz. This signal is digitized with a sampling rate of the order of 100 MHz from which the field vector is calculated. The resulting field vector of each cavity is multiplied by a rotation matrix to calibrate amplitude and phase. The vector sum of the 32 cavity fields represents the total voltage and phase seen by the beam. Errors in the calibration can result in residual voltage fluctuations in the presence of microphonics while the measured vector sum is held constant. The measured vector sum is subtracted from the setpoint table, and the resulting error signal is amplified and filtered to provide a feedback signal to the vector modulator controlling the incident wave. A feedforward signal is added to correct the averaged repetitive error components. Beam current information (measured by toroids) is used to scale the feedforward table to provide fast feedforward corrections if the beam current varies. The cavity detuning is determined from forward power, reflected power and probe signal and is used to control the fast piezotuners to reduce detuning errors to less than a tenth of the cavity bandwidth.

5. RF control software architecture

The RF control software shown in figure 3 consists of the following.

- User interface (operator displays).
- Control system functionality (display editor, history and archive, database, data acquisition system).
- Application servers.
- Adaptive feedforward.
- System identification (including automation server).
- Measurement and control algorithms (field measurement and field calibration, loop phase and loop gain, feedback controller, cavity resonance control).

6. RF vector from the sampled IF signal

If IQ sampling is applied (the usual sequence is $+I, +Q, -I, -Q$), the field vector is given by the I and Q values [9]. Measurement offsets are corrected by calculating I and Q from the average of the positive and negative values. In the case of near IQ sampling [10], it is possible to correct for down-converter nonlinearities by averaging over many points over the IF signal period. In near IQ sampling the measurements are spaced in time by nearly 90° in RF phase to ensure that amplitude and phase can be detected with good accuracy with only a few samples. Look-up tables for sin and cos are required to correct for the deviations from IQ sampling. Taking samples near IQ support fast and precise amplitude and phase measurements from only a few samples.

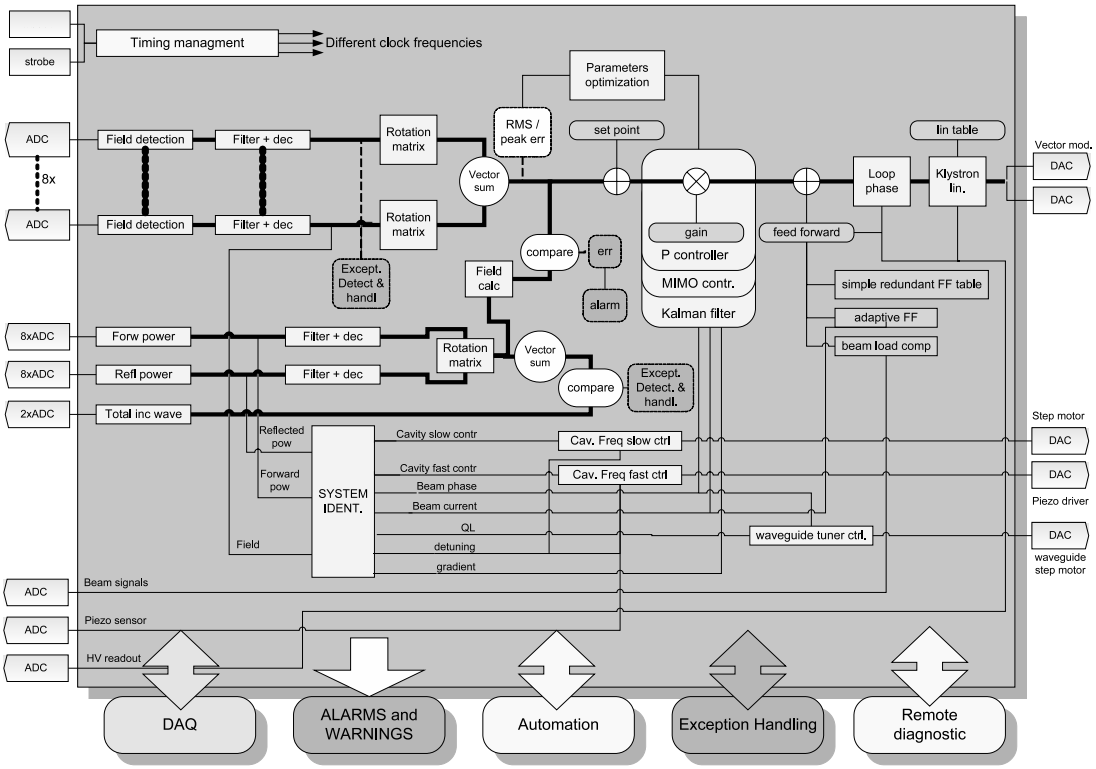

Figure 3. Software architecture and signal flow.

For given parameters for the IF frequency f_{IF} and the ADC clock f_{clck}, the field vector is given by [9]

$$I = \frac{2}{N}\sum_{i=0}^{N-1} x_i \sin(i\alpha) \tag{1}$$

$$Q = \frac{2}{N}\sum_{i=0}^{N-1} x_i \cos(i\alpha), \tag{2}$$

where x_i are the samples of the signal, N is the number of samples and $\alpha = 2\pi \cdot f_{\mathrm{IF}}/f_{\mathrm{clck}}$ is the phase advance between subsequent samples.

Typical examples of vector measurements are shown in figure 4.

7. Loop phase and loop gain measurement

The loop phase characterizes the phase offset in the feedback loop and can be described as the sum of the system phase shift and the phase shift through the feedback controller:

$$\Phi_L = \Phi_{\mathrm{sys}} - \Phi_{\mathrm{ctrl}}, \tag{3}$$

where Φ_{sys} is the system phase shift between the vector-modulator input and the measured vector sum and Φ_{ctrl} is the phase shift across the controller.

The system phase depends on the electrical length of the various cables and amplifiers in the forward and measurement path and will change as a function of the high voltage of the klystron (14° kV^{-1}) as well as phase drifts due to temperature changes. Relevant for control purposes is the dynamic phase shift since the digital control system will have to correct errors by step changes in the drive and will react on time scales

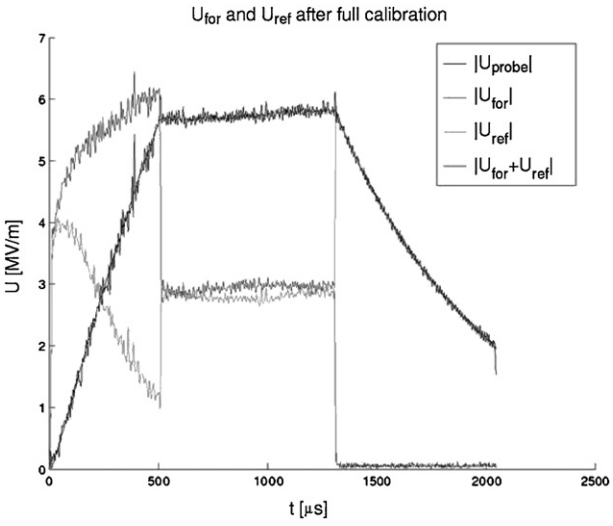

Figure 4. Measurement of the amplitudes of probe signal, forward power and reflected power.

which are small compared to the time constant of the cavity. Therefore, the system phase is measured as the difference of the phase angles between the vector sum and the drive vector in the transient case. An example for the loop phase measurement is shown in figure 5. The measurement shows that the changes in loop phase are strongly correlated with the SASE intensity. A possible source of the loop phase change is changes in the high voltage of the klystron and/or temperature change of the waveguide distribution system.

The system gain is defined as the ratio of the amplitudes of the measured vector sum and drive vectors for the steady

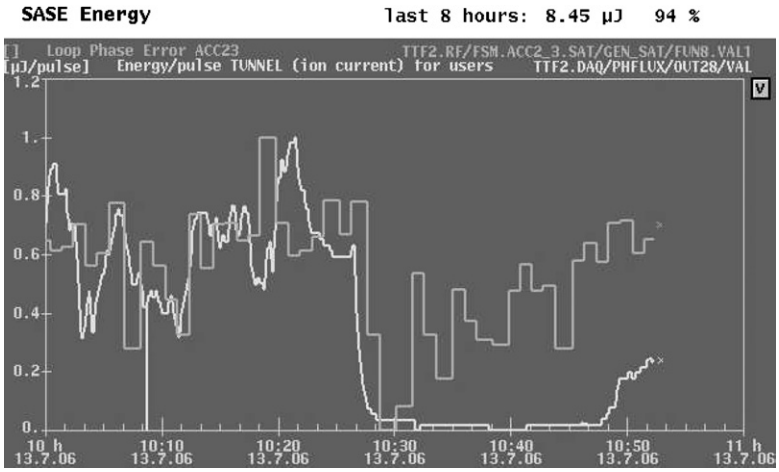

Figure 5. Measurement of loop phase and correlation with the SASE intensity

state case when the cavity is operated on resonance. It will change as a function of the klystron power due to the klystron saturation characteristics.

8. Loaded Q and cavity detuning

The loaded Q and cavity detuning are parameters in the differential equation:

$$\begin{pmatrix} \dot{v}_r \\ \dot{v}_i \end{pmatrix} = \begin{pmatrix} -\omega_{12}(t) & -\Delta\omega(t) \\ +\Delta\omega(t) & -\omega_{12}(t) \end{pmatrix} \begin{pmatrix} v_r \\ v_i \end{pmatrix} + \cdots \omega_{12}(t) \left(\frac{r}{q}\right) \frac{1}{2} \cdot \omega_0 \begin{pmatrix} 1 & 0 \\ 0 & 1 \end{pmatrix} \begin{pmatrix} I_r \\ I_i \end{pmatrix}, \tag{4}$$

where

$$\omega_{12} = \frac{\omega_0}{2Q_{\mathrm{L}}(t)} \qquad \text{and} \qquad \left(\frac{I_r}{I_i}\right) = \left(\frac{I_r}{I_i}\right)_{\mathrm{kly}} + \left(\frac{I_r}{I_i}\right)_{\mathrm{beam}}. \tag{5}$$

As in the case of the loop gain and loop phase which form a vector, the cavity loaded Q and detuning also form a complex vector with loaded Q as the real part and cavity detuning as the imaginary component.

$$\dot{\vec{v}} = -(\omega_{12} - \mathrm{i}\Delta\omega)\,\vec{v} + \frac{1}{2}\omega_0 \left(\frac{r}{Q}\right)(\vec{I}_{\mathrm{kly}} + \vec{I}_{\mathrm{beam}}). \tag{6}$$

The loaded Q and cavity detuning can be measured during the field decay where the driving term is turned off. An example of a cavity detuning measurement is shown in figure 6. This figure shows a comparison of the detuning measured by pulse shortening and a single pulse measurement using system identification methods.

9. Cavity phase and gradient

The initial coarse gradient calibration can be achieved using the klystron power calibration. With known losses in the power transmission system including waveguides, couplers and circulator, the power to individual cavities will be known with an accuracy of ±10%. Knowing the shunt impedance

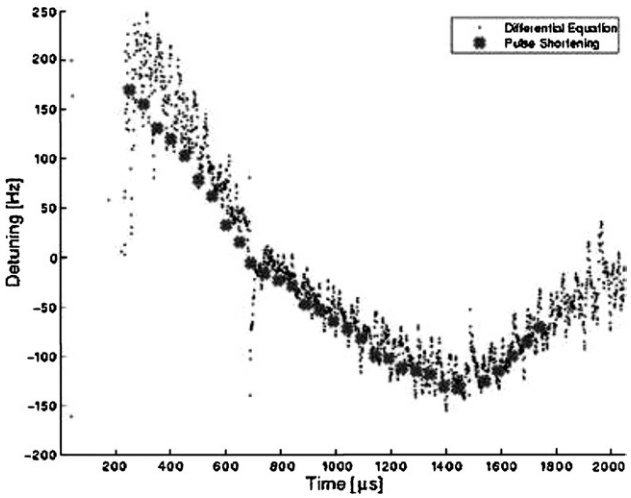

Figure 6. Cavity detuning measurement solving the differential equation and with pulse length scan where the detuning is measured at the beginning of the field decay.

r/Q and the loaded Q_{L} (from the field decay), the steady state gradient induced by the klystron can be estimated as

$$V_{\mathrm{kly}} = 2\sqrt{\left(\frac{r}{Q}\right) Q_{\mathrm{L}} P_{\mathrm{kly}}}. \tag{7}$$

The precise gradient calibration and the calibration with respect to the beam can be accomplished only with reference to the beam-induced voltage. This can be done with short beam pulses (transient detection) or long beam pulses (steady state full beam loading). The more beam loading is available, the better is the accuracy of the measurement.

9.1. Transient beam loading

The magnitude of the transient induced by a single bunch is given by

$$|V_{\mathrm{bunch}}| = \left(\frac{r}{Q}\right) Q_{\mathrm{L}} \cdot I \frac{\Delta t}{\tau} = \left(\frac{r}{Q}\right) \frac{Q_b \omega_0}{2}. \tag{8}$$

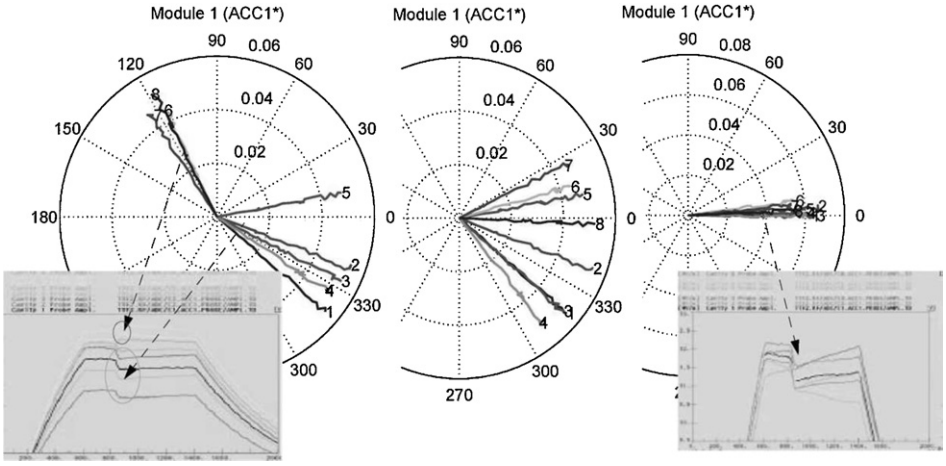

Figure 7. Transient detection applied to the adjustment of the incident phase. The transient portion is shown in the polar plots which show the result of the progressive tuning of the incident phase from left to right.

If the bunch charge is not known precisely, one still can calibrate the gradients with respect to each other (assuming that the shunt impedance is known precisely) and calibrate the total energy gain with the spectrometer. The phase of the transient signal with respect to the phase of the cavity voltage determines the beam phase. Since the transient of a 1 nC bunch is of the order of 2×10^{-4} at 25 MV m^{-1}, the measurement of the transient with a few per cent accuracy requires a resolution of better than 1×10^{-5} for a gradient of the order of 25 MV m^{-1}. Currently, a measurement accuracy of 10° for phase can be achieved with a single 1 nC pulse. Averaging over several hundred measurements is necessary to achieve the required precision of 0.5° for the European XFEL. An example of the transient-based measurements is shown in figure 7.

9.2. Full beam loading

With full beam loading and under (quasi-) steady state conditions, the beam phase and beam-induced voltage for zero cavity detuning can be determined from

$$\vec{V}_{\mathrm{kly}} = 2\sqrt{\left(\frac{r}{Q}\right) Q_{\mathrm{L}}}\,\vec{V}_{\mathrm{inc}} \tag{9}$$

and

$$\vec{V}_{\mathrm{beam}} = \left(\frac{r}{Q}\right) Q_{\mathrm{L}} \vec{I}_{\mathrm{beam}} \tag{10}$$

with

$$\vec{V}_{\mathrm{cav}} = \vec{V}_{\mathrm{inc}} - \vec{V}_{\mathrm{ref}}, \tag{11}$$

where $\vec{V}_{\mathrm{cav}}, \vec{V}_{\mathrm{inc}}$ and $\vec{V}_{\mathrm{ref}}$ are measured and calibrated quantities. In the presence of cavity detuning and/or transient behaviour, corrections must be applied or the differential equation must be solved The expected accuracy can be of the order of 1° for phase and 1% in amplitude for a 800 μs beam pulse at full beam current.

9.3. Spectrometer-based measurement

The gradient and phase calibration should be cross checked using a spectrometer for the measurement of the beam energy. If the relative gradient calibration between cavities is known (the same beam current is in all cavities if the beam loss is small), one can calibrate individual gradients if the total energy is known. The overall crest phase can be verified by the measurement of the beam energy as a function of the linac phase and can be determined with a good accuracy of the order of 1° depending on the resolution of the spectrometer.

10. Vector sum

With the individual cavity gradients calibrated in amplitude and phase, the vector sum can be calculated as

$$\vec{V}_{\mathrm{sum}} = \sum_{i=1}^{32} \vec{V}_i^{\mathrm{cal}} = \sum_{i=1}^{32} \vec{V}_i^{\mathrm{raw}} \begin{pmatrix} a & b \\ -b & a \end{pmatrix}_i^{\mathrm{rot}}. \tag{12}$$

Errors in the calibration of the vector sum will limit the achievable field regulation in the presence of microphonics.

10.1. Beam phase and beam current

Since the beam loading is used to calibrate the cavity gradient and phase with respect to the beam, the calibrated cavity fields can be used to determine the beam current and phase. Inconsistencies with toroid and beam phase measurements can be used to flag inconsistencies in the calibration.

11. Exception detection

Exceptions can be derived as deviations from the standard behaviour of signals or system parameters.

11.1. Quench detection

A cavity quench or thermal breakdown can be detected as a significant drop in the unloaded quality factor Q_0 which affects the loaded quality factor Q_{L}. Since Q_{L} is given by

$$\frac{1}{Q_{\mathrm{L}}} = \frac{1}{Q_0} + \frac{1}{Q_{\mathrm{ext}}} \qquad \text{i.e.} \qquad Q_0 = \frac{Q_{\mathrm{ext}} \cdot Q_{\mathrm{L}}}{Q_{\mathrm{ext}} - Q_{\mathrm{L}}}, \tag{13}$$

an unloaded Q drop to 3×10^8 could be detected if the resolution of the loaded Q measurement is 1% for a loaded Q of $Q_{\mathrm{L}} = 3 \times 10^6$.

12. Error detection

Errors are detected as deviations of signals from the expected value and can result in warnings or alarms. Other error types are rms fluctuations of gradient and phase during the flat-top portion of the pulse since they determine the expected beam energy stability or longitudinal bunch profile. The errors can be interpreted as exceptions and may require exception handling procedures to recover from the error state.

13. Conclusion

A modern LLRF control system requires detailed information about a large number of signals and parameters in the RF system. This demand can be fulfilled with the measurement of a large number of physically available signals. A good model of the LLRF system allows the derivation of the desired signals and parameters. The high data rates require powerful data processing engines and communication links which are readily available in the form of FPGAs, DSPs and CPUs, Gigabit Ethernet and optical Gigalinks.

Acknowledgments

I acknowledge the support of the European Community-Research Infrastructure Activity under the FP6 'Structuring the European Research Area' programme (CARE, contract number RII3-CT-2003-506395).

References

[1] Schilcher T 1998 Vector sum control of pulsed accelerating fields in Lorentz force detuned superconducting cavities *PhD Thesis* University of Hamburg

[2] Brinkmann R 2004 Accelerator layout of the XFEL *LINAC04 (Lübeck, Germany, 16–20 August)*

[3] The European X-Ray Free-Electron Laser *Technical Design Report* May 2006, http://xfel.desy.de

[4] Brinkmann R, Flottmann K, Rossbach J, Schmüser P, Walker N and Weise H 2001 *Technical Design Report Part II—The accelerator* (Deutsche Elektronen-Synchrotron DESY, 2001)

[5] Simrock S N, Cichalewski W, Grecki M K, Jablonski G W and Jalmuzna W J 2006 Universal controller for digital RF control *Proc. EPAC 2006* pp 1459–61

[6] Giergusiewicz W *et al* 2005 Low latency control board for LLRF system: SIMCON 3.1 *Proc. SPIE (Photonics Applications in Industry and Research IV)* vol 5948 pp 710–5

[7] Simrock S N 2004 State of the art in RF control *Proc. 2004 LINAC Conf. (Lübeck, Germany)* pp 523–5

[8] Ayvazyan V, Rehlich K and Simrock S N 2003 Requirements for RF control of TTF II FEL user facility *Proc. 2003 Particle Accelerator Conf.* pp 2342–4

[9] Grecki M, Jezynski T and Brandt A 2005 Estimation of IQ vector components of RF field—theory and implementation *12th Int. Conf. Mixed Design of Integrated Circuits and Systems (MIXDES 2005)* pp 783–8

[10] Doolittle L, Ma H and Champion M 2006 Digital low-level RF control using non-IQ sampling *Proc. LINAC 2006* pp 568–70